

$\text{PPh}_2)_2\text{Rh}(\text{COD})$ should be half the number in $[\text{Rh}(\mu\text{-PPh}_2)(\text{COD})]_2$, if both COD ligands are lost from the latter. The rate of hydrogenation of 1-octene with $[(\text{DPPE})\text{Rh}(\mu\text{-PPh}_2)_2\text{Rh}(\text{COD})]$ is actually greater than the rate for $[\text{Rh}(\mu\text{-PPh}_2)(\text{COD})]_2$ (Table IV), and the effective catalyst life is much longer for $[(\text{DPPE})\text{Rh}(\mu\text{-PPh}_2)_2\text{Rh}(\text{COD})]$. The increased rate is apparently due to the increased basicity of the complex on coordination of the diphosphine ligand,^{31d} and the longer catalyst life is due probably to a greater stability of the DPPE portion of the complex, which diminishes side reactions that deactivate the catalyst.

With bimetallic complexes or clusters, the possibility always exists for cleavage to a monometallic species that becomes the actual catalyst. Thus, to test our assumption that DPPE did not dissociate readily from the "mixed" COD-DPPE complex $[(\text{DPPE})\text{Rh}(\mu\text{-PPh}_2)_2\text{Rh}(\text{COD})]$, we examined the H_2 catalyst activity of $[\text{Rh}(\mu\text{-PPh}_2)(\text{DPPE})]_2$. Unfortunately, the results obtained with the latter complex are somewhat ambiguous; clearly, the complex is not active at ambient conditions for approximately 3 h, in contrast to immediate catalysis by $[(\text{DPPE})\text{Rh}(\mu\text{-PPh}_2)_2\text{Rh}(\text{COD})]$; however, after 3 h under H_2 , solutions containing $[\text{Rh}(\mu\text{-PPh}_2)(\text{DPPE})]_2$ begin to hydrogenate 1-octene at a rate comparable to that of $\text{RhCl}(\text{PPh}_3)_3$. The nonactivity for the first 3 h suggests that the dimer is not cleaved rapidly to a monomer and that DPPE dissociation is slow. The activity observed for $[\text{Rh}(\mu\text{-PPh}_2)(\text{DPPE})]_2$ after 3 h may result from a slow dissociation of DPPE to produce an intermediate that can coordinate and then hydrogenate the olefin substrate. Even after the 3-h induction period, the rate of hydrogenation by $[\text{Rh}(\mu\text{-PPh}_2)(\text{DPPE})]_2$ is slower than the rate for $[(\text{DPPE})\text{Rh}(\mu\text{-PPh}_2)_2\text{Rh}(\text{COD})]$; the slower rate may be due to competition between the olefin and the dissociated DPPE ligand for coordination sites on rhodium. These data suggest that the bimetallic nature of the complexes in Table IV is retained

during hydrogenation and that cleavage of the phosphido bridges does not occur to produce the active catalyst in solution.³⁴

Acknowledgment. We are grateful to the OSU Small Grants Program and Johnson Matthey Co. for partial financial support of this research and to the National Science Foundation (Grant No. CHE-7910019) and the National Institutes of Health (Grant No. GM-27431) for recent instrumentation grants that aided the purchase of the 300- and 200-MHz NMR instruments, respectively. We also thank Professor G. G. Christoph for help with the X-ray structure determination and the John Simon Guggenheim Foundation for a fellowship to D.W.M. for 1981-1982.

Registry No. $[\text{Ir}(\mu\text{-PPh}_2)(\text{CO})(\text{PPh}_3)]_2$, 39732-63-3; Ph_2PH , 829-85-6; $\text{IrCl}(\text{CO})(\text{PPh}_3)_2$, 14871-41-1; $[\text{Ir}(\mu\text{-PPh}_2)(\text{COD})]_2$, 83681-88-3; $[\text{Ir}(\mu\text{-Cl})(\text{COD})]_2$, 12112-67-3; $[\text{RhCl}(\text{COD})]_2$, 12092-47-6; $\text{Rh}_2(\mu\text{-Cl})(\mu\text{-PPh}_2)(\text{COD})_2$, 83681-89-4; $[\text{Rh}(\mu\text{-PPh}_2)(\text{COD})]_2$, 82829-24-1; $[\text{Rh}(\mu\text{-PPh}_2)(\text{DPPM})]_2$, 83681-90-7; $[\text{Rh}(\mu\text{-PPh}_2)(\text{DPPE})]_2$, 83681-91-8; $[\text{Rh}(\mu\text{-PPh}_2)(\text{DPPP})]_2$, 83681-92-9; $[\text{Rh}(\mu\text{-PPh}_2)(\text{Arphos})]_2$, 83681-93-0; $(\text{PEt}_3)_2\text{Rh}(\mu\text{-PPh}_2)_2\text{Rh}(\text{COD})$, 83681-94-1; $(\text{PMePh}_2)_2\text{Rh}(\mu\text{-PPh}_2)_2\text{Rh}(\text{COD})$, 82847-79-8; $[\text{Rh}(\mu\text{-PPh}_2)(\text{Ph}_2\text{PCH}=\text{CHPPh}_2)]_2$, 83681-95-2; $[\text{Rh}(\mu\text{-PPh}_2)(\text{Ph}_2\text{PCH}_2\text{CH}_2\text{PEtPh})]_2$, 83681-96-3; $\text{Rh}_2(\mu\text{-PPh}_2)_2(\text{DPPM})(\text{COD})$, 83681-97-4; $\text{Rh}_2(\mu\text{-PPh}_2)_2(\text{DPPE})(\text{COD})$, 83681-98-5; $\text{Rh}_2(\mu\text{-PPh}_2)_2(\text{DPPP})(\text{COD})$, 83681-99-6; $\text{Rh}_2(\mu\text{-PPh}_2)_2(\text{Ph}_2\text{PCH}_2\text{CH}_2\text{PEtPh})(\text{COD})$, 83682-00-2; $\text{Rh}_2(\mu\text{-PPh}_2)_2(\text{PPH})(\text{COD})$, 83682-01-3; $(\text{Ph}_3\text{P})_2\text{Rh}(\mu\text{-PPh}_2)_2\text{Rh}(\text{COD})$, 82847-80-1; $(\text{Cy}_3\text{P})_2\text{Rh}(\mu\text{-PPh}_2)_2\text{Rh}(\text{COD})$, 83682-02-4; $\text{RhCl}(\text{PPh}_3)_3$, 14694-95-2; 1-octene, 111-66-0; cyclohexene, 110-83-8; 2,3-dimethylbut-2-ene, 563-79-1.

(34) In view of Carty's recent results under catalytic hydrogenation conditions,²⁵ one should be cautious about extrapolating the noncleavage of the $\mu\text{-PPh}_2$ group under hydrogen at 1 atm pressure to higher temperatures and pressures of H_2 .

Contribution from the Department of Chemistry,
Washington State University, Pullman, Washington 99164

Crystal Structure and Magnetic Properties of $\text{Cu}_2\text{Cl}_2(\text{C}_5\text{H}_5\text{N})_2(\text{OCH}_3)_2$: A Catalytic Species Related to the Copper(II)-Induced Oxidation of Phenols

R. D. WILLETT and G. L. BRENNAN*

Received April 29, 1982

The crystal structure of a catalytic precursor in the oxidation of phenols, $\text{Cu}_2\text{Cl}_2(\text{C}_5\text{H}_5\text{N})_2(\text{OCH}_3)_2$, has been determined. The unit cell is triclinic, space group $P\bar{1}$, with $a = 8.280(3) \text{ \AA}$, $b = 6.089(2) \text{ \AA}$, $c = 9.302(5) \text{ \AA}$, $\alpha = 62.67(2)^\circ$, $\beta = 94.67(3)^\circ$, and $\gamma = 70.81(2)^\circ$. The structure consists of methoxy-bridged dimers connected to each other through asymmetric chlorine bridges, forming a one-dimensional chain. The copper coordination sphere is distorted square pyramidal. The Cu-O distances are 1.932(4) and 1.940(6) \AA , the intradimer Cu-Cu distance is 3.037(2) \AA , and the bridging Cu-O-Cu angle is 103.2(1)°. Magnetic susceptibility studies indicate antiferromagnetic coupling within dimers in the solid state with a singlet-triplet splitting of 1030 K. The implications of this with respect to mechanisms of exchange coupling are discussed. The EPR spectrum is characteristic of an exchange-coupled system. The g values are consistent with the observed stereochemistry.

Introduction

It is known that copper(I) chloride in pyridine/methanol in the presence of oxygen catalyzes the oxidation of phenols and catechols.¹ It has been suggested that this represents a nonenzymatic model reaction for oxygenases such as pyro-

catechase.^{2,3} The four-electron oxidation of catechol to *cis,cis*-muconic acid, monomethyl ester, proceeds with equal

- (1) (a) A. S. Hay, H. S. Blanchard, G. F. Endres, and J. W. Eustance, *J. Am. Chem. Soc.*, **81**, 6335 (1959); (b) A. S. Hay, *J. Polym. Sci.*, **58**, 581 (1962); (c) G. F. Endres and J. Kwiatek, *ibid.*, **58**, 593 (1962); (d) G. F. Endres, A. S. Hay, and J. W. Eustance, *J. Org. Chem.*, **28**, 1300 (1963); (e) A. S. Hay and G. F. Endres, *J. Polym. Sci., Part B*, **3**, 887 (1965); (f) H. Finkbeiner, A. S. Hay, H. S. Blanchard, and G. F. Endres, *J. Org. Chem.*, **31**, 549 (1966).

* To whom correspondence should be addressed at the Department of Chemistry, Eastern Washington University, Cheney, WA 99004.

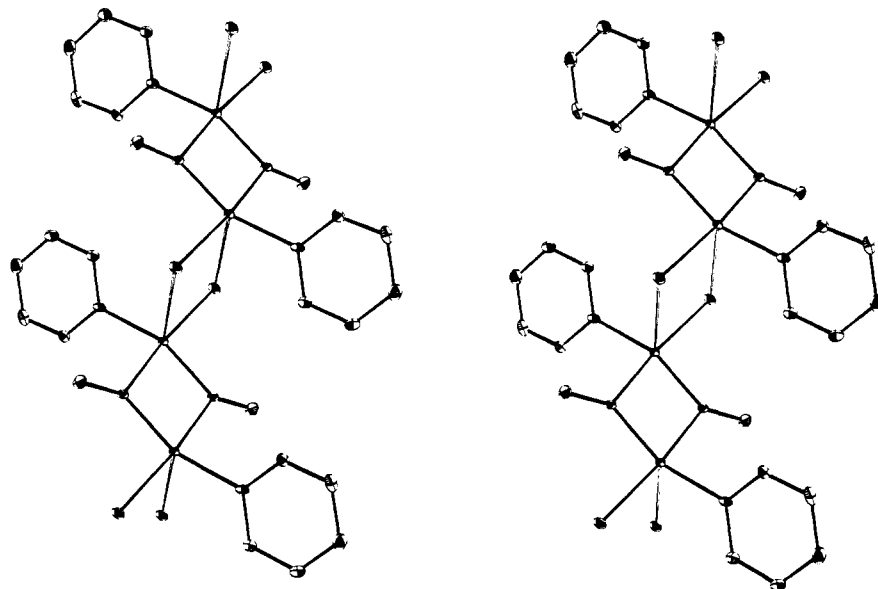


Figure 1. Illustration of the structure of Cu₂Cl₂(C₅H₅N)₂(OCH₃)₂.

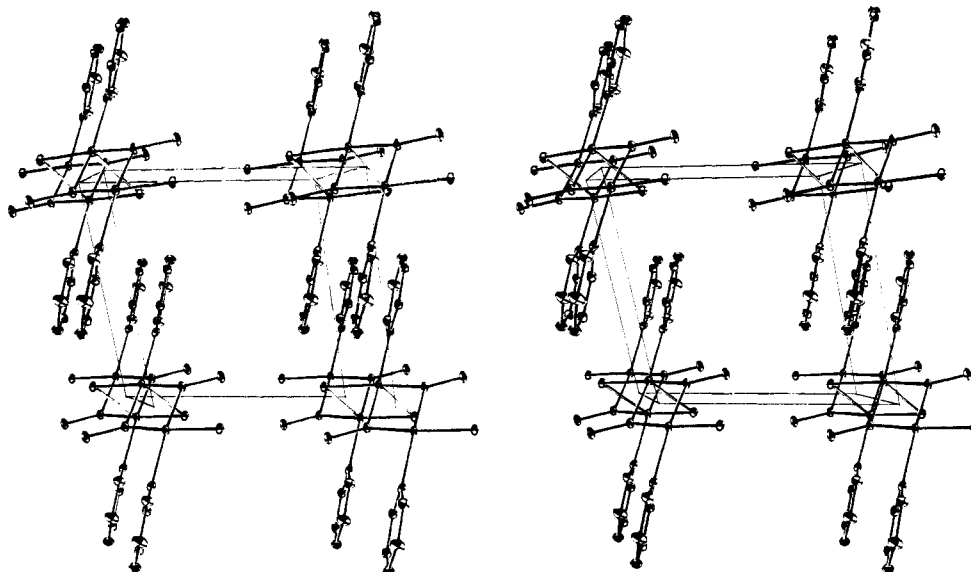


Figure 2. Stereographic view of the unit cell contents of Cu₂Cl₂(C₅H₅N)₂(OCH₃)₂.

facility under anaerobic conditions in the presence of copper(II).⁴

In a detailed study by Rogic and Demmin,⁴ it has been shown that the process actually occurs as a pair of two-electron oxidation processes, generating the stable intermediate *o*-benzoquinone. Further, it was shown that the reagent can be generated by dissolving Cu(OMe)₂ with H₂O in pyridine and is equivalent to a dimeric [Cu(OMe)(OH)Cu]²⁺ species complexed with pyridine. It can be generated in a number of different ways, including the dissolution of Cu(py)(OMe)Cl in pyridine. The chloride ion plays an essential role in the regeneration of the reagent, in that a CuCl₂ species scavenges the final oxidation product, which otherwise ties up the Cu(I) and prevents its reoxidation. The overall oxidation clearly involves electron transfer from the substrate to the active copper reagent, which later transfers electrons to molecular

oxygen. Thus, no activation of molecular oxygen occurs.

We have initiated a study of the role of cluster compounds in catalytic processes. As part of this study, we have undertaken the determination of the crystal structure of Cu(py)(OMe)Cl. The results of this analysis are reported in this paper.

Experimental Section

Single crystals of the compound were prepared by modifying the procedure of Finkbeiner, Hay, Blanchard, and Endres.⁵ A 0.5-g quantity of CuCl₂ and 2 mL of pyridine were placed in 150 mL of dry methanol. This mixture was placed in a desiccator for several days to allow atmospheric O₂ to slowly diffuse into the solution, giving a slow crystal growth. Dark green needles resulted.

Weissenberg and precession photographs showed $\bar{1}$ symmetry and no systematic absences. A set of 12 accurately centered reflections yielded the following lattice constants ($\lambda(\text{Mo K}\alpha) = 0.71069 \text{ \AA}$): $a = 8.280(3) \text{ \AA}$, $b = 6.089(2) \text{ \AA}$, $c = 9.302(5) \text{ \AA}$, $\alpha = 62.67(2)^\circ$, $\beta = 94.67(3)^\circ$, and $\gamma = 70.81(2)^\circ$. Data were collected on a Picker diffractometer by using the θ - 2θ scan technique with Zr-filtered Mo K α radiation. Each scan was 2.6° in 2θ with a counting time of 3.5 s/0.05 $^\circ$ step. A 17.5-s background was measured at the beginning

- (2) J. Tsuji and H. Takayanagi, *J. Am. Chem. Soc.*, **96**, 7349 (1974); (b) J. Tsuji, H. Takayanagi, and I. Sakai, *Tetrahedron Lett.*, 1245 (1975).
 (3) Cf. for example G. A. Hamilton in "Molecular Mechanism of Oxygen Activation", O. Hayaishi, Ed., Academic Press, New York, 1974, p 405, and references therein.
 (4) M. M. Rogic, T. R. Demmin, W. B. Hammond, *J. Am. Chem. Soc.*, **98**, 7441 (1976); M. M. Rogic and T. R. Demmin, *ibid.*, **100**, 5472 (1978).

- (5) H. Finkbeiner, A. S. Hay, H. S. Blanchard, and G. F. Endres, *J. Org. Chem.*, **31**, 549-555 (1966).

Table I. Positional and Thermal Parameters in $\text{CuCl}(\text{OCH}_3)(\text{C}_5\text{H}_5\text{N})^c$

(A) Non-Hydrogen Atoms ^b									
atom	x	y	z	β_{11}	β_{22}	β_{33}	β_{12}	β_{13}	β_{23}
Cu	0026 (1)	2180 (2)	0898 (1)	0081 (2)	0154 (5)	0106 (2)	-0077 (2)	0011 (1)	-0056 (2)
Cl	-1917 (2)	0337 (4)	0713 (2)	0115 (4)	0274 (10)	0135 (4)	-0128 (5)	0041 (3)	-0111 (5)
O	1472 (6)	4113 (9)	0878 (6)	0080 (10)	0151 (23)	0131 (9)	-0062 (12)	0013 (7)	-0071 (12)
N	1473 (8)	9076 (12)	3234 (7)	0124 (13)	0196 (30)	0121 (11)	-0117 (16)	0049 (10)	-0083 (16)
C(1)	3350 (12)	2930 (22)	1283 (14)	0079 (17)	0257 (45)	0200 (20)	-0069 (23)	0013 (14)	-0085 (27)
C(2)	2034 (12)	6421 (16)	3682 (11)	0182 (19)	0241 (42)	0139 (16)	-0104 (23)	0008 (14)	-0090 (22)
C(3)	1829 (10)	9580 (17)	4447 (10)	0121 (18)	0275 (44)	0126 (16)	-0094 (23)	0026 (13)	-0107 (23)
C(4)	2925 (14)	4387 (19)	5302 (12)	0262 (26)	0204 (43)	0177 (19)	-0115 (27)	-0032 (17)	-0054 (25)
C(5)	2700 (11)	7633 (20)	6062 (11)	0137 (18)	0522 (58)	0121 (17)	-0159 (26)	0031 (14)	-0149 (27)
C(6)	3283 (12)	4909 (20)	6544 (11)	0186 (21)	0377 (50)	0114 (16)	-0147 (27)	0009 (14)	-0049 (24)

(B) Hydrogen Atoms^a

atom	x	y	z	B, Å ²	atom	x	y	z	B, Å ²
H(1A)	37 (2)	18 (3)	10 (2)	5 (4)	H(3)	13 (1)	15 (2)	40 (1)	0 (1)
H(1B)	36 (1)	46 (3)	06 (2)	3 (3)	H(4)	36 (1)	25 (2)	55 (1)	3 (2)
H(1C)	37 (1)	36 (3)	19 (2)	4 (3)	H(5)	28 (1)	78 (2)	69 (1)	1 (2)
H(2)	15 (1)	65 (1)	26 (1)	0 (2)	H(6)	37 (1)	36 (2)	77 (1)	3 (2)

^a Positional parameters are multiplied by 10^2 . ^b All entries are multiplied by 10^4 . ^c Uncertainties are given in parentheses.

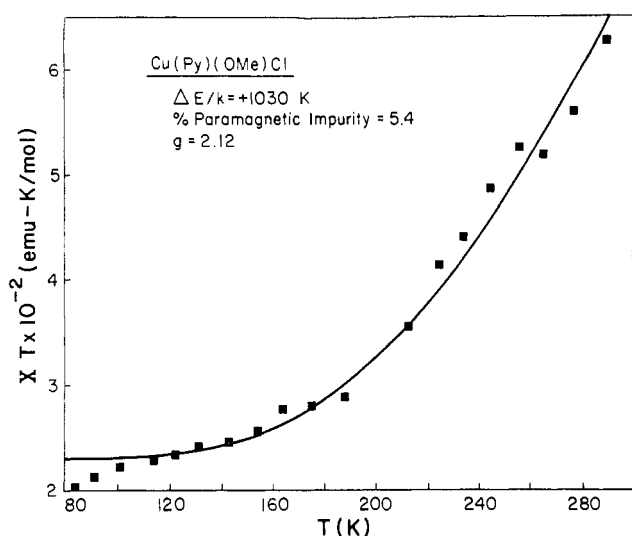


Figure 3. Magnetic susceptibility of $\text{Cu}_2\text{Cl}_2(\text{C}_5\text{H}_5\text{N})_2(\text{OCH}_3)_2$. The solid line is the least-squares fit to eq 1 with $\Delta E/k = +1030$ K and $\alpha = 0.054$.

and end of each scan. A total of 1093 independent reflections were measured. Absorption corrections were applied ($\mu = 32.87 \text{ cm}^{-1}$). The Cu positions were found on a Patterson map and used to calculate structure factor signs for an electron-density map. This map showed the remaining non-H atom positions. Least-squares refinement then routinely proceeded (with H atoms added toward the end) to give $R = 0.066$, where $R = \sum ||F_o| - |F_c|| / \sum |F_o|$. Scattering factors were taken from ref 6. Final parameters are listed in Table I, and a list of observed and calculated structure factors is given in Table II (supplementary material). Relevant interatomic distances and angles are reported in Table III, and the structure is illustrated in Figures 1 and 2. Crystallographic programs utilized included locally modified versions of ORFLS3, ORFEE3, ORABS, ORTEP, and ALFF.

Magnetic Studies

Magnetic susceptibility data, shown in Figure 3, were measured on a PAR vibrating-sample magnetometer. The data were indicative of strong antiferromagnetic coupling, with essentially a zero moment at 80 K. After correction for the diamagnetism and temperature-independent paramagnetism terms, the product χT assumed a nearly constant, nonzero value for temperatures below 80 K. The extrapolated value of χT at $T = 0$ corresponded to approximately 5% impurity. Indication of further antiferromagnetic coupling between the impurity ions was evident at very low temperatures. Thus, only data above

Table III. Interatomic Distances (Å) and Angles (deg)^a

Cu Coordination Sphere and Intradimer Interactions			
Cu-Cl	2.279 (3)	Cu-N	2.012 (5)
Cu-O	1.932 (4)	O-O ^b	2.402 (8)
Cu-O ^b	1.940 (6)	Cu-Cu ^b	3.037 (2)
Cl-Cu-O	173.9 (1)	N-Cu-Cl	93.6 (2)
Cl-Cu-O ^b	95.7 (2)	O-Cu-O ^b	76.7 (2)
N-Cu-O ^b	157.9 (3)	Cu-O-Cu ^b	103.2 (1)
N-Cu-O	92.0 (2)		
Interdimer Interactions			
Cu-Cl ^c	2.820 (3)	Cl-Cl ^c	3.512 (4)
Cu-Cu ^c	3.736 (3)		
Cl ^c -Cu-O	97.2 (2)	Cl ^c -Cu-N	94.3 (2)
Cl ^c -Cu-O ^b	105.5 (2)	Cu-Cl-Cu ^c	93.62 (8)
Cl ^c -Cu-Cl	86.38 (8)		
Ligands			
O-C(1)	1.41 (1)	C(6)-C(5)	1.39 (1)
N-C(2)	1.36 (1)	C(5)-C(3)	1.34 (1)
C(2)-C(4)	1.36 (1)	C(3)-N	1.33 (1)
C(4)-C(6)	1.36 (1)		
Cu-O-C(1)	123.4 (6)	C(2)-C(4)-C(6)	121.7 (9)
Cu ^b -O-C(1)	124.2 (6)	C(4)-C(6)-C(5)	116.4 (8)
Cu-N-C(2)	123.0 (6)	C(6)-C(5)-C(3)	120.0 (9)
Cu-N-C(3)	119.7 (5)	C(5)-C(3)-N	123.7 (8)
N-C(2)-C(4)	121.0 (8)	C(3)-N-C(2)	117.2 (7)
Carbon-Hydrogen			
C(1)-H(1A)	0.8 (2)	C(3)-H(3)	0.95 (7)
C(1)-H(1B)	1.0 (1)	C(4)-H(4)	1.02 (12)
C(1)-H(1C)	0.9 (1)	C(5)-H(5)	0.81 (9)
C(2)-H(2)	1.03 (7)	C(6)-H(6)	0.96 (9)

^a Uncertainties given in parentheses. ^b Atom related by $\bar{x}, \bar{y}, \bar{z}$. ^c Atom related by $\bar{x}, 1 - y, \bar{z}$.

80 K were used for the analysis. In light of the structural results (vide infra), the data were fit to a simple dimer model, with a contribution allowed for the paramagnetic impurity:

$$\chi = (1 - \alpha) \frac{C_1}{T} \frac{1}{1 + \frac{1}{3} \exp(\Delta E/kT)} + \alpha \frac{C_{1/2}}{T} \quad (1)$$

where ΔE is the singlet-triplet splitting energy (positive ΔE implying singlet low), $C_{1/2}$ and C_1 are the Curie constants for spin $1/2$ and spin 1 systems, respectively, and α is the fraction impurity. This gave a good fit to the experimental data with $\Delta E/k = 1030$ K with 5.4% impurity.

The EPR spectrum of a powder sample was measured on a Varian E-3 spectrometer. It is a typical powder spectrum for an anisotropic g tensor but with no hyperfine structure. The g values are approximately $g_x = 2.06$, $g_y = 2.08$, and $g_z = 2.22$. Also, no absorption was observed at half-field corresponding to a $\Delta M = \pm 2$ line characteristic

(6) "International Tables for Crystallography", Vol. III, Kynoch Press, Birmingham, England, 1962.

of an isolated dimer. Thus, the spectrum is representative of an extended exchange-coupled system. Interdimer interaction frequencies then must be greater than the EPR frequency.

Discussion

As proposed by Finkbeiner et al.,¹ our title compound exists as discrete dimers which, however, stack to form linear chains in the solid state. Within the centrosymmetric dimers, the copper(II) ions are linked together by a pair of methoxy ions with symmetrical Cu–O–Cu bridges. The bridging bond distances (Cu–O = 1.932 and 1.940 Å; Cu–O–Cu = 103.2°) are normal, as is the geometry around each copper (Cu–N = 2.012 Å; Cu–Cl = 2.279 Å). The Cu₂O₂Cl₂ framework is essentially planar, but the nitrogen atoms lie out of that plane. In addition the py ring is twisted 86° with respect to that plane to give efficient stacking of the py rings (see Figure 2). The methoxide carbon (C(1)) lies substantially off the Cu₂O₂ plane (0.64 Å).

The interdimer packing is such that the chloride ion of one dimer occupies the fifth coordination site of a copper in the adjacent dimer. This produces the not unusual 4 + 1 coordination geometry for each copper, with the axial Cu–Cl distance (2.820 Å) being significantly larger than the equatorial Cu–Cl distances. As is usual in these systems, the axial Cu–Cl distance is apparently dictated by ligand–ligand repulsive forces, with no distances between the axial Cl and the equatorial ligands being shorter than the sum of the van der Waals radii.⁷ Thus, these chloride bridges are asymmetrical and lead to an interdimer Cu–Cu distance of 3.736 Å. The Cu–Cl–Cu bridging angle at 93.62° is slightly larger than 90°.

Recently, the structures and magnetic properties of a substantial number of alkoxy-bridged copper dimers (or aggregations of copper dimers) have been reported.^{8–12} In particular, it has been shown¹⁰ that a linear relationship exists between the bridging Cu–O–Cu angle and the magnitude of the singlet–triplet splitting, ΔE , and is very similar to that found by Hatfield, Hodgson, and co-workers in the hydroxy-bridged copper dimers.¹³ The slope of the line relating ΔE to the bridging angle is the same in both series.¹⁰ However, the angle for which $\Delta E = 0$ is smaller for the alkoxy series (95.7°) than for the hydroxy series (97.6°). Our data are

consistent with those of the other alkoxy-bridged species, with the observed value of the singlet–triplet separation (1030 K) lying slightly above the value predicted by the assumed linear relation (~880 K). The predicted value for the hydroxy-bridged series is substantially smaller (~600 K). It has been shown by Hay, Thibeault, and Hoffmann¹⁴ that replacing the OH⁻ bridging ligand by a more electronegative group such as OR⁻ (R = alkyl) should lead to an increase in the strength of the antiferromagnetic interaction. The experimental results appear to be in good experimental accord with their predictions.

In solution, it is likely that Cu(py)(OMe)Cl exists in multiple equilibria with other species. One possible such species is a dimer configuration involving methoxy or hydroxy bridges, with the fifth and sixth coordination sites of each copper being occupied by solvent molecules. It is thus possible to visualize the four-electron oxidation process to occur in a pair of two-electron oxidative processes as proposed by Rogic et al.⁴ In the first step, the substrate binds to an axial coordination site on one or both copper atoms of the dimer; sequential one-electron steps then oxidize the phenol or catechol to the quinone while successively reducing the two copper ions to Cu(I). The second process involves a similar coordination of the quinone to a second dimer, with corresponding one-electron oxidations causing C–C bond cleavage.

Finkbeiner et al.¹ also identified a species (py)₄Cu₄Cl₆O, which exhibited limited catalytic activity. It was readily isolated from ethanol or propanol solutions but only obtained with great difficulty from methanol. We have also isolated this species and by crystallographic analysis shown it to be identical with the material of the same formula whose structure was determined by Kilbourn and Dunitz.¹⁵ This is a cluster compound, with each copper ion exhibiting a trigonal-bipyramidal coordination with the chlorine and oxygen atoms bridging to other copper atoms in the cluster. If, as is likely, the tetramer dissolves as a cluster in solution, its lower catalytic activity with respect to Cu(py)(OMe)Cl is readily understood since the copper ions are now coordinately saturated and the substrate would have to displace a pyridine molecule from the cluster to initiate the catalysis steps.

Acknowledgment. This work was supported by the NSF. Assistance of Dr. C. P. Landee, Mr. G. Needham, and R. Gaura in the collection of the magnetic data is gratefully acknowledged.

Registry No. Cu₂Cl₂(C₅H₅N)₂(OCH₃)₂, 29057-95-2.

Supplementary Material Available: Table II, showing observed and calculated structure factors (3 pages). Ordering information is given on any current masthead page.

- (7) R. D. Willett and K. Chang, *Inorg. Chim. Acta*, **4**, 447 (1970).
- (8) J. E. Andrew and A. B. Blake, *J. Chem. Soc., Dalton Trans.*, 1102 (1973); 447 (1976).
- (9) R. Mergehenn, L. Merz, and W. Haase, *J. Chem. Soc., Dalton Trans.*, 1703 (1980).
- (10) L. Merz and W. Haase, *J. Chem. Soc., Dalton Trans.*, 875 (1980), and references therein.
- (11) B. Jezowska-Trzebiatowska, Z. Olejnik, and T. Lis, *J. Chem. Soc., Dalton Trans.*, 251 (1981).
- (12) L. Banci, A. Bencini, P. Dapporto, A. Dei, and D. Gatteschi, *Inorg. Chem.*, **19**, 3395 (1980).
- (13) V. H. Crawford, H. W. Richardson, J. R. Wasson, D. J. Hodgson, and W. E. Hatfield, *Inorg. Chem.*, **15**, 2107 (1976).

(14) P. J. Hay, J. C. Thibeault, and R. Hoffmann, *J. Am. Chem. Soc.*, **97**, 4884 (1975).

(15) B. T. Kilbourn and J. D. Dunitz, *Inorg. Chim. Acta*, **1**, 209 (1967).